HAL
open science

Trapping, cooling, and photodissociation analysis of state-selected H_2^+ ions produced by (3+1) multiphoton ionization

Julian Schmidt, Thomas Louvradoux, Johannes M Heinrich, Nicolas Sillitoe, Malcolm Simpson, Jean-Philippe Karr, Laurent Hilico

▶ **To cite this version:**

Julian Schmidt, Thomas Louvradoux, Johannes M Heinrich, Nicolas Sillitoe, Malcolm Simpson, et al.. Trapping, cooling, and photodissociation analysis of state-selected H_2^+ ions produced by (3+1) multiphoton ionization. Physical Review Applied, 2020, 14 (2), 10.1103/PhysRevApplied.14.024053 . hal-02561042v2

HAL Id: hal-02561042

https://hal.science/hal-02561042v2

Submitted on 25 Aug 2020

HAL is a multi-disciplinary open access archive for the deposit and dissemination of scientific research documents, whether they are published or not. The documents may come from teaching and research institutions in France or abroad, or from public or private research centers.

L'archive ouverte pluridisciplinaire **HAL**, est destinée au dépôt et à la diffusion de documents scientifiques de niveau recherche, publiés ou non, émanant des établissements d'enseignement et de recherche français ou étrangers, des laboratoires publics ou privés.

Trapping, cooling, and photodissociation analysis of state-selected H_2^+ ions produced by (3+1) multiphoton ionization

Julian Schmidt[1], Thomas Louvradoux[1], Johannes Heinrich[1], Nicolas Sillitoe[1], Malcolm Simpson[2], Jean-Philippe Karr[1,3], and Laurent Hilico[1,3]
[1]*Laboratoire Kastler Brossel, Sorbonne Université, CNRS, ENS-PSL Research University, Collège de France 4 place Jussieu, F-75005 Paris, France*
[2]*Institut für Ionenphysik und Angewandte Physik, Universität Innsbruck, Technikerstraße 25, 6020 Innsbruck, Austria and*
[3]*Université d'Evry-Val d'Essonne, Université Paris-Saclay, Boulevard François Mitterrand, F-91000 Evry, France*
(Dated: August 25, 2020)

We report on the production of cold, state-selected H_2^+ molecular ions in a linear RF trap. The ions are produced by (3+1) resonance-enhanced multi-photon ionisation (REMPI) of H_2, and sympathetically cooled by laser-cooled Be^+ ions. After demonstrating and characterizing the REMPI process, we use photodissociation by a deep UV laser at 213 nm to verify the high vibrational purity of the produced H_2^+ ion samples. Moreover, the large difference between the photodissociation efficiencies of ions created in the $v = 0$ and $v = 1$ levels provides a way to detect a $v = 0 \rightarrow 1$ transition. These results pave the way towards high-resolution vibrational spectroscopy of H_2^+ for fundamental metrology applications.

I. INTRODUCTION

Precision spectroscopy of hydrogen molecular ions (HMI) is a promising method to improve the determination of fundamental constants [1]. By measuring several well-chosen rovibrational transitions in both H_2^+ and HD^+, it is possible to determine the m_p/m_e and m_d/m_e mass ratios, the proton and deuteron charge radii and the Rydberg constant [2]. In particular, the present theoretical uncertainty of rovibrational transition frequencies in HMI, which is at a few parts-per-trillion level [3], allows for significant progress in the determination of m_p/m_e [4, 5]. H_2^+ also has strong potential for ultra high resolution spectroscopy at the 10^{-17} level for tests of the time independence of m_p/m_e [6, 7].

So far, dipole-allowed rovibrational transitions have been measured in sympathetically cooled HD^+ ion ensembles with 1-2 ppb accuracies, limited by Doppler broadening [8–10]. More recently, a pure rotational transition was measured in the Lamb-Dicke regime with a 0.38 ppb accuracy [11, 12], and a two-photon vibrational transition was measured with a 2.9 ppt uncertainty [13].

Spectroscopy of the homonuclear species H_2^+ poses additional challenges in comparison to HD^+, due to the fact that rovibrational transitions are dipole-forbidden. In the case of HD^+, the ions may be simply produced by electron-impact ionization, after which spontaneous decay to the ground vibrational state occurs within a few hundreds of milliseconds. The population of a rotational state of interest for spectroscopy can be further increased using rotational cooling methods [9, 14] or exploiting rotational transitions induced by blackbody radiation (BBR) [10, 15]. In H_2^+, due to the very long lifetimes of rovibrational levels in the 10^6 s range [16], ions created by electron-impact remain scattered in many rovibrational states, which strongly limits the achievable spectroscopic signal [17]. In addition, methods relying on optical pumping or BBR-induced transitions are not available.

One possible way of producing H_2^+ ion ensembles in a pure rovibrational state is to create the ions by electron impact, and achieve rovibrational cooling through collisions with a cold He buffer gas [18], as recently analyzed theoretically by S. Schiller and coworkers [19–21]. They estimated that cooling to the vibrational ground state, in competition with loss of molecules through the reaction $H_2^+ + He \rightarrow HeH^+ + H$, should occur within a time of about 10 s, and that rotational cooling within the $v = 0$ state is feasible within approximately 40 s for a He density of 10^9 cm^{-3}. Since collisions with He do not affect the nuclear spin, in order to get a single rotational state one should in addition start from para-H_2 gas using an ortho-para H_2 converter, or remove ions in the unwanted $L = 0$ (para) or $L = 1$ (ortho) state by resonance-enhanced multiphoton dissociation (REMPD).

In this paper, we demonstrate an alternative method relying on state-selective production of H_2^+ by four-photon (3+1) resonance-enhanced multiphoton ionization (REMPI) of H_2 [22]. We report on the production, trapping, and sympathetic cooling of state-selected H_2^+ ions in $v = 0$ and $v = 1$. A similar idea has been used to produce cold, state-selected N_2^+ ions by threshold ionization [23]. This work is an important step towards our goal of performing high-resolution spectroscopy of the $(v = 0, L = 2) \rightarrow (v' = 1, L' = 2)$ Doppler-free two-photon transition [17]. The transition will be detected by REMPD, similarly to previous experiments in HD^+, using a 213 nm laser to selectively dissociate ions excited to the $v = 1$ level. Here, we use photodissociation to verify the vibrational selectivity of the REMPI process. Moreover, we show that the $v = 1$ level is dissociated much more efficiently than $v = 0$, confirming the pos-

sibility of detecting a $v = 0 \rightarrow v' = 1$ transition via REMPD.

The paper is organized as follows: after describing the experimental setup in Sec. II, we characterize REMPI H_2^+ ion production in the vibrational states $v = 0$ and $v = 1$ in Sec. III. The sympathetic cooling of the state-selected H_2^+ ions, is addressed in Sec. IV, where we also describe a nondestructive method to measure the ion number. Finally, experimental results of state-selective photodissociation of H_2^+ are presented and analyzed in Sec. V.

II. EXPERIMENTAL SETUP

The experimental setup consists of a pulsed H_2 molecular beam apparatus (Fig. 1(a)) which can be connected to two different ultrahigh vacuum (UHV) chambers, one containing a hyperbolic RF ion trap (Fig. 1(b)) and the other one a linear RF ion trap (Fig. 1(c)). A pulsed, tunable laser with a wavelength near 300 nm (called "REMPI laser" in the following) can be used to create H_2^+ ions by REMPI in either trap.

A. H_2 molecular beam

The molecular beam is produced by a fast pulsed piezo valve (Amsterdam Piezo Valve) with a 150 μm nozzle and a 5-10 μs opening time from a reservoir with a stagnation pressure of 1.5 bar. The beam passes through a first skimmer with aperture 1 mm, located 6.3 cm from the nozzle, and a second skimmer with aperture 150 μm, located 20.5 cm from the nozzle. The pulsed valve chamber is evacuated with a CF160 high compression ratio turbo pump. The chamber between the two skimmers is evacuated using a CF63 turbo pump and an ion-getter pump in order to maintain ultrahigh vacuum conditions in the ion trap chamber. An all-metal gate valve allows for separating the molecular beam chamber and mounting it to either the hyperbolic ion trap chamber or to the linear ion trap chamber. The two traps are described in more detail below. The distance between the nozzle and the trap center ("flight distance" in Fig. 1(a)) is 62(1) cm for the hyperbolic trap and 65(1) cm for the linear trap. Finally, the orientation of the molecular beam with respect to the ion trap can be adjusted by means of a universal joint (not shown in Fig. 1) placed between the second skimmer (S_2) and the gate valve.

B. Hyperbolic trap

The hyperbolic trap [17] is made of stainless steel with a ring of inner radius $r_0 = 4.2$ mm and two endcaps separated by $2z_0 = 6$ mm. It is operated with an RF voltage amplitude of 180 V at 13.4 MHz and DC voltage of 1 V between the ring and endcap electrodes. The upper and lower endcap electrodes feature along the y axis, respectively, a 1 mm hole for electron injection from a home-made electron gun polarized at -150 V, and a 3 mm hole for ion extraction and detection on a microchannel plate. The H_2 molecular beam and the REMPI laser beam are perpendicular to each other, and respectively aligned with the x and z direction. They enter the trap along two pairs of 5 mm holes drilled in the ring electrode.

C. Linear trap

The segmented linear trap is made of four cylindrical molybdenum rods of 4 mm radius and 36 mm length, and the distance from the trap axis to the electrodes is $r_0 = 3.5$ mm. Two diagonally opposing rods are segmented into 12 mm long parts. The trap is operated with an RF amplitude of up to 550 V at 13.3 MHz and a DC voltage up to 8 V between the central part and ends of the segmented rods, allowing for trapping of both H_2^+ and Be^+. The Be^+ ions are created via electron-impact ionization of a neutral Be effusive beam coming from a ceramic Be oven described in [32]. A Be wire (length 5 mm, diameter 0.25 mm) is inserted in a four hole ceramic tube (tube diameter 1.2 mm, hole diameter 0.254 mm) heated by a 0.25 mm diameter tantalum wire wound through the three other holes. The Be oven is located at 46 mm from the trap center. The Be effusive beam is collimated by a 1 mm diaphragm located at 25 mm from the oven resulting in a 20 mrad beam half-angle and a beam diameter of about 2 mm at the trap center. The oven current is 3 A, slightly above the threshold current (2.9 A) to observe Be^+ ions in the trap. An electron gun (Kimball Physics FRA-2X1-2) is installed with a 20 mm working distance from the trap center. The electron gun filament is polarized at -110 V with respect to ground potential, and the filament current is set to 1.4 A to have a 10 μA emission current. Note that due to the RF electric field in the trap, the electron beam energy and spot size cannot be known precisely. The oven and electron gun are oriented symetrically with respect to the vertical y axis, making a 25 degree angle with it and aiming at the trap center (see Fig. 1(c)). To create Be^+ ions in the trap, both the oven and electron gun are turned on for 30 s and then turned off. The typical trapping voltages are 470 V RF amplitude, 0 V on the central segment and 8 V on the endcap segments resulting in a stability parameter $q_x = 0.12$ and the secular frequencies $f_x = f_y = 550$ kHz in the x and y directions and f_z =126 kHz in the z direction for Be^+.

The Be^+ cooling laser at 313 nm is aligned with the trap axis z. The REMPI laser is counterpropagating with respect to the cooling laser and is aligned using diaphragms centered on the cooling laser beam. The dissociation laser (described and used in Sec. V) propagates in the $x - z$ plane with an angle of 28.5° with respect to the trap axis. The H_2 molecular beam enters the trap along the x axis. The fluorescence of the Be^+ ions is imaged on an electron multiplying charge-coupled device

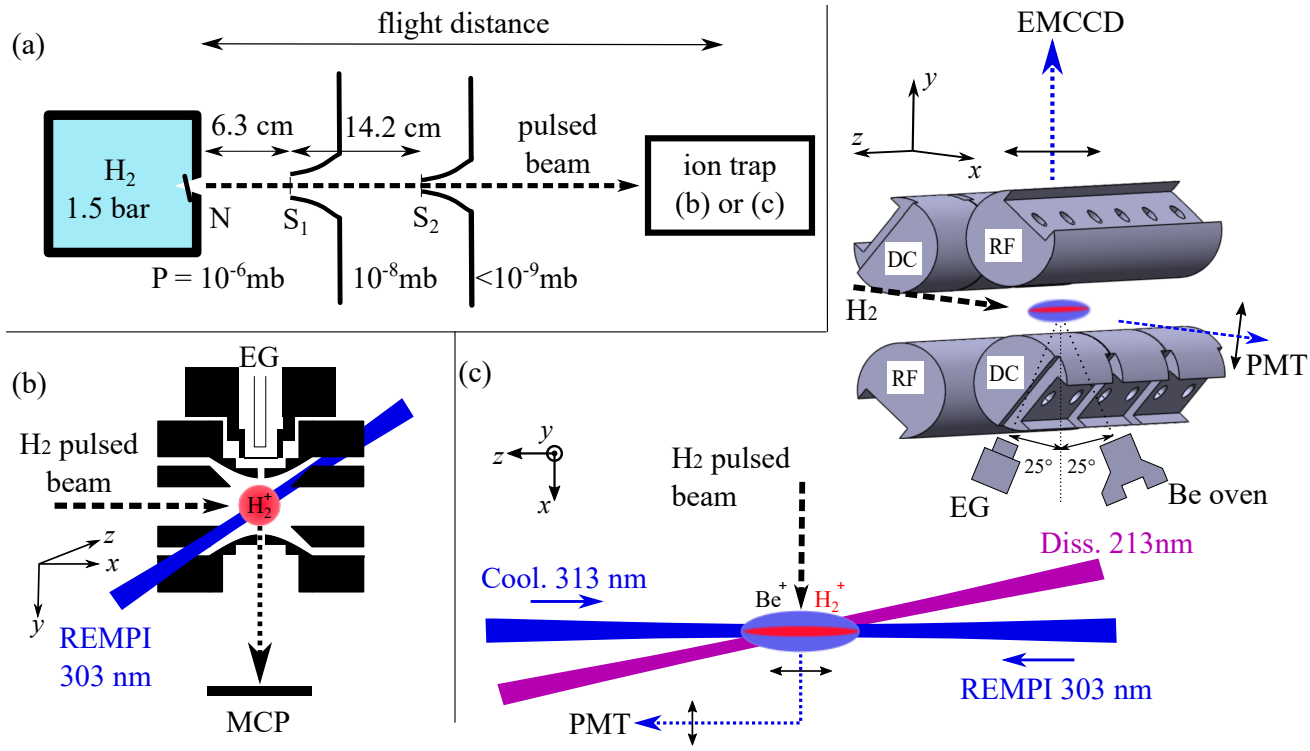

FIG. 1: Schematic of the experimental setups. (a) The molecular beam setup, which can be connected to one of two UHV chambers containing different ion traps. N: pulsed valve with a 150 μm nozzle, S_1: 1 mm skimmer, S_2: 150 μm skimmer. Typical pressures in the different pumping stages are indicated. The pressures in the ion traps are typically 10^{-10} mbar. (b) Hyperbolic RF ion trap. EG: electron gun (home-made tungsten hair pin), MCP: microchannel plate. (c) Segmented linear RF ion trap with laser-cooled Be^+ ions. EG: Kimball Physics electron gun FRA-2X1-2. Imaging of the Be^+ fluorescence on the EMCCD camera is done using a $f = 70$ mm objective with a magnification of 9. Another part of the fluorescence is collected by an in-vacuum lens ($f = 30$ mm) and focused on a photomultiplier tube (PMT).

(EMCCD) camera along the vertical y axis and focused on a photomultiplier tube (PMT) along the horizontal x axis. The background pressure in both trap chambers is of the order of 10^{-10} mbar.

D. REMPI laser

The REMPI laser is a frequency-doubled pulsed dye Laser (Sirah Precision scan) pumped with a Q-switched YAG laser with a repetition rate of 20 Hz and a pulse energy of 110 mJ. We get about 4 mJ at 303 nm using an optimized mix of rhodamine 610 (64%) and rhodamine 640 (36%) with 0.12 g/l total concentration in ethanol, and 3 mJ at 296 nm using pure rhodamine 610. The elliptical beam profile is circularized using cylindrical lenses. It has a divergence of 1.6 mrad and an M^2 factor of about 2.

III. CREATION OF H_2^+ IONS BY REMPI

Creation of hydrogen molecular ions from the pulsed H_2 molecular beam (Fig. 1(a)) by REMPI was first tested and optimized in the absence of sympathetic cooling, using the hyperbolic rf trap (Fig. 1(b)). With this trap, production yields can be easily measured by extracting the ions towards a multichannel plate detector. In addition, the experimental cycle is shorter (about 7 s) than in the linear trap (about 45 s) since it does not include the preparation of a cold Be^+ crystal. This makes the hyperbolic trap well suited to measure the REMPI spectrum and optimize the molecular beam and laser parameters.

(3+1) REMPI of H_2 is a two-step process consisting of a resonant three-photon excitation to a given rovibrational state of the Rydberg $C^1\Pi_u$ electronic state, followed by nonresonant one-photon ionization. It thus requires tight focusing of the REMPI laser. The laser beam is expended to a diameter of about 12 mm and focused with a $f = 189$ mm spherical lens. A spot diameter of about 12 μm is expected, but the Rayleigh length $Z_R = 0.2$ mm is small as compared to the molecular beam diameter at the trap center or to the precision of the focal spot localization along the beam axis. The effective beam diameter in the interaction region is thus larger than 12 μm. The very small ion production volume leads to low ionization yields, and precise overlap of the REMPI beam with both the trap center and the

molecular beam is mandatory in order to observe a signal. Overlap with the trap center is achieved using the photodissociation of H_2^+ ions created by electron-impact ionization. This process populates a large number of vibrational levels (from $v = 0$ to 12) [24], and a significant fraction of the produced ions is efficiently dissociated at 303 nm. The beam is then aligned with the trap center by maximizing the fraction of photodissociated ions, after which the focal point is located at the center by *minimizing* the photodissociated fraction. Finally, the electron gun is turned off and the molecular beam is aligned with the trap center using the universal joint mentioned in Sec. II, in order to optimize the REMPI signal.

Spectra of the REMPI process near 303 nm and near 296 nm, are shown in Fig. 2 and are in good agreement with previous results [25]. The signal in the $v = 1$ state is weaker due to several reasons: reduced laser power, different transition strengths and possible dissociation of the ions it produces. The $v = 1$ photodissociation cross section at 296 nm is $2.18\times10^{-26}\mathrm{m}^2$ [24] leading to the dissociation of up to 80% of the produced ions for 3 mJ, 7 ns pulses focused with a 12 μm spot diameter. The $v = 1$ signal is only suppressed by a factor of two, which indicates that the spot diameter of 12 μm is underestimated and that the effective diameter is at least two times larger. We observe an asymmetry and a broadening of the lines with an FWHM of about 0.1 nm. We attribute them to the AC Stark shift of the intermediate C state of H_2 [26, 27]. An upper bound of this shift is given by the ponderomotive shift of the loosely bound electron at the center of the beam,

$$\frac{q^2\lambda^2 E}{4\pi^3\epsilon_0 m c^3 w_0^2 \tau} = 8.7\,\mathrm{meV}, \qquad (1)$$

where q is the elementary charge, m the electron mass, $w_0 = 6$ μm and where $E = 4$ mJ and $\tau = 7$ ns are the typical pulse energy and duration. This corresponds to a 0.64 nm shift in terms of wavelength, which is significantly larger than the observed maximum shift, indicating again that the effective beam diameter is at least two times larger than expected.

For the experiments described in the following, we tune the wavelength to 302.47 nm or 295.61 nm to produce ions in the $v = 0$ or the $v = 1$ state via the combination of the (unresolved) R(0) and R(1) lines.

Fig. 3 shows the dependence of the REMPI signal on the pulse energy. The data is in good agreement with a cubic law, indicating that only the ionization step from the C state is saturated but not the three-photon transition rate. Saturation of the REMPI process was observed by another group using a pulse energy of approximately 20 mJ [28].

Fig. 4 shows the dependence of the REMPI signal on the delay between the opening of the pulsed valve and the laser pulses. The optimum observed for $\Delta t_{\mathrm{tof}} = 282(1)\,\mu$s, for the 62(1) cm distance between the nozzle and the trap (see Fig. 1), corresponds to a most probable velocity of $v_{mp} = 2190(40)$ m/s. The initial pulse duration is difficult to access experimentally. By observing the drive voltage of the pulsed valve, we estimate it to be shorter than 10 μs. Neglecting this duration, the mea-

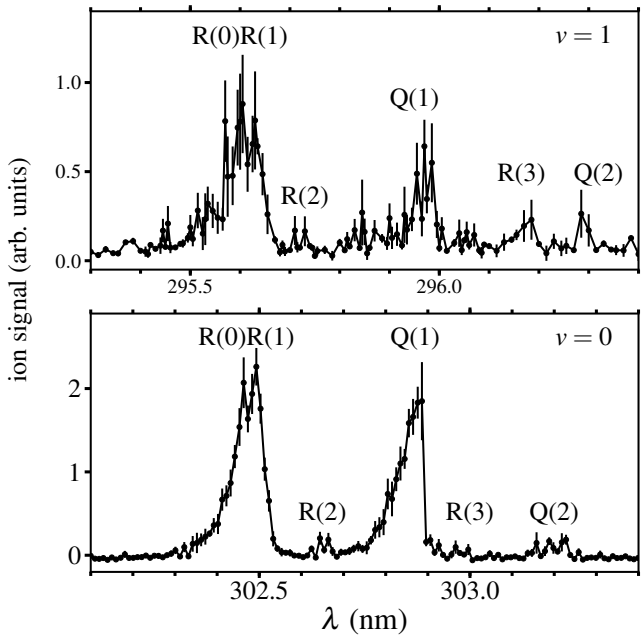

FIG. 2: Mean ion signal as a function of the REMPI laser wavelength, obtained after 3 s of REMPI pulses synchronized with H_2 pulses (corresponding to 60 pulses). The ion signal is averaged over 10 to 20 experimental cycles. Error bars represent the standard deviation. The positions of the resonances are in good agreement with the data shown in [25], allowing their identification.

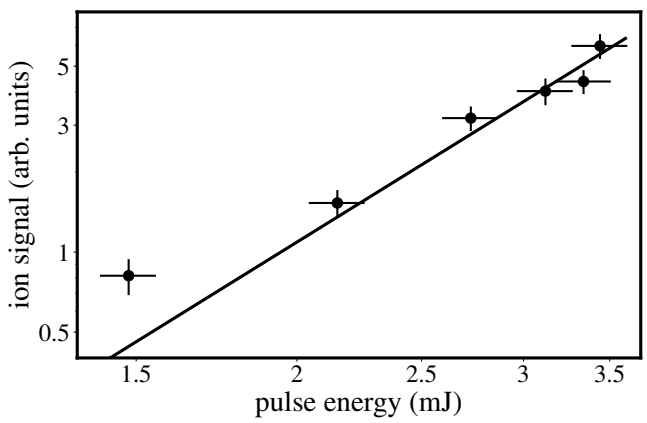

FIG. 3: Mean ion signal from the $v = 0$, R(0)-R(1) line (see Fig. 2) as a function of pulse energy. Each data point is an average of 10 to 60 experiments. Horizontal error bars represent a 5% uncertainty of the pulse energy. Vertical error bars include the statistical deviation within one measurement run and a conservative estimate of the stability over the duration of the entire experiment. The stability is in part limited by the fluctuating H_2 background gas pressure. The solid line is a fit with a cubic model, ion signal $= 0.136\,E^3$.

sured FWHM of 35(2) μs after expansion corresponds to a velocity dispersion smaller than $\delta v = 271(15)$ m/s. These values indicate that the molecular beam is operated in an intermediate regime between an effusive beam, for which $v_{mp} = 1906$ m/s and $\delta v = 1780$ m/s, and a supersonic beam, for which $v_{mp} = \sqrt{7RT_0/M} = 2900$ m/s (for a diatomic molecule) with a narrow velocity distribution [29] . In the latter formula, R is the molar gas constant, M the molar mass and T_0 the room temperature.

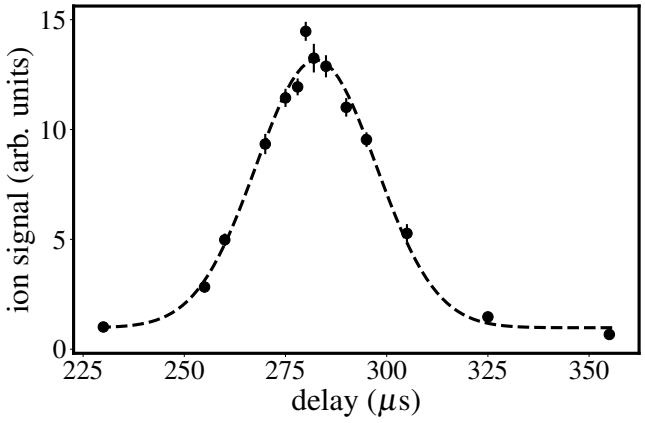

FIG. 4: Mean ion signal in the $v = 0$ state as a function of the time of flight, i.e. the delay between the opening of the pulsed valve and the REMPI laser pulse. Each data point is the average of 10 to 20 experimental sequences. Error bars represent the standard deviation. The backing pressure is 2 bar and the valve opening duration is estimated to be shorter than 10 μs. The dashed line is a fit by a Gaussian function with a FWHM of 35(2) μs.

During injection of the pulsed molecular beam, the pressure in the ion trap chamber remains at an acceptably low value. After a 3 s REMPI cycle, corresponding to 60 gas pulses, it increases by about 1. 10^{-10} mbar for a few seconds. Over tens of experimental cycles, the pressure eventually increases to a few 10^{-10} mbar. We believe this stems from a slow increase of the pressure in the intermediate vacuum sections of the molecular beam apparatus (see Fig.1) rather than from the gas flux of the H_2 pulses themselves. Faster pumping of the intermediate vacuum may alleviate this issue. We also note that using pure para-H_2 would allow the amount of injected gas to be reduced by a factor of three.

IV. SYMPATHETIC COOLING OF STATE-SELECTED IONS AND ION COUNTING

After testing state-selective production with the hyperbolic trap, we now use the linear rf trap where the H_2^+ ions produced by REMPI can be sympathetically cooled by laser-cooled Be^+ ions [30, 31].

The experimental sequence begins by creating a Coulomb crystal of several hundred Be^+. The ions are produced as explained in section II and laser cooled at a detuning of about $5\Gamma = 2\pi\times$ 100 MHz and an intensity of about $1 \times I_{\rm sat}$=0.83 mW/mm^2. The cooling laser at 313 nm is obtained by sum frequency mixing of two fiber lasers at 1051 and 1549 nm amplified up to 4.5 W and cavity enhanced second harmonic generation in a Brewster-cut 12 mm long BBO non-linear crystal [33].

Ionic species heavier than Be^+ are also created by the electron impact process from atoms or molecules evaporated from the Be oven. These are washed out of the trap by adding for 1 s a DC component of about 9V to the RF voltage, which makes singly charged ions of mass $\geq$10 unstable. The RF voltage amplitude is then reduced to 340 V to lower the q stability parameter to 0.09 and the secular frequency to $f_x = 400$ kHz for Be^+, in order to keep H_2^+ stability parameter below 0.4.

Next, the pulsed molecular beam, synchronized with the REMPI laser, is turned on for a variable time between $0.5\,\mathrm{s} < t_c < 3\,\mathrm{s}$ to create state-selected H_2^+ ions. The focusing of the REMPI laser slightly differs from Sec. III: the beam is expanded to about 16 mm and focused using a $f = 236$ mm lens, which again results in an expected spot diameter of about 12 μm. After the pulsed laser is turned off, we observe dark ions embedded in the Coulomb crystal, see Fig. 5(a).

The dark ion species can be identified by exciting their secular motion in the trap and observing the corresponding effect on the fluorescence of the Be^+ ions. This signal also provides a way to measure nondestructively the number of trapped H_2^+ ions, which will be used for the REMPD spectroscopy of H_2^+, as done in previous experiments on HD^+, see e.g. [8, 10, 15]. In practice, an AC voltage is applied to one of the trap electrodes and its frequency is swept linearly with time. When only Be^+ is trapped, we observe an increase in the fluorescence rate near $f_{\rm sec,Be^+} = 400$ kHz. After REMPI and when dark ions are present, we observe a peak near $4.5 \times f_{\rm sec,Be^+} = 1800$ kHz, indicating the presence of H_2^+, see Fig. 5(b). An additional peak appears near 1200 kHz after 10-20 s, which we attribute to the formation of H_3^+ through the reaction $H_2^+ + H_2 \rightarrow H_3^+ + H$. The observed H_3^+ formation rate is proportional to the H_2^+ ion number and is consistent with a partial H_2 pressure of about 5×10^{-10} mbar [34]. The area under the peak can be assumed, as a reasonable approximation, to be proportional to the number of H_2^+ ions, as analyzed in detail in [15].

V. PHOTODISSOCIATION OF STATE-SELECTED, SYMPATHETICALLY COOLED H_2^+ IONS

The study of photodissociation of the H_2^+ ions created by REMPI serves two purposes. Firstly, due to the strong dependence of the photodissociation cross-section on the vibrational state, the photodissociation dynamics gives information on the vibrational population distribution,

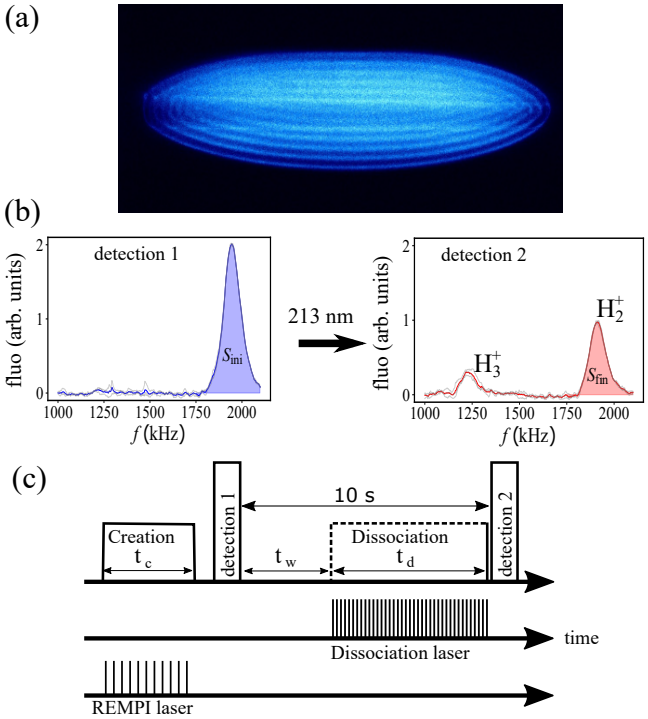

FIG. 5: Sympathetic cooling and detection of H_2^+ ions produced by REMPI. (a) Fluorescence image of a Be^+ ion Coulomb crystal in the linear trap. The dark region along the horizontal axis is due to the presence of sympathetically cooled H_2^+ ions. (b) Typical detection signals of H_2^+ ions. The fluorescence of the Be^+ ions is measured as a function of the excitation frequency f. Three 0.5 s sweeps (light grey) are averaged. The peak at about 1.8 MHz corresponds to excitation of the radial secular motion of H_2^+. In the second signal, the peak around 1.2 MHz corresponds to the appearance of H_3^+ ions due to chemical reactions of H_2^+ with H_2 (see text). The H_2^+ ion signal is the shaded area below the curve. (c) Experimental sequence for measuring the photodissociation efficiency. The H_2^+ ion number is measured non-destructively before and after interaction with the 213 nm laser.

and thus allows us to check the vibrational selectivity of the REMPI process. Secondly, we will show evidence of the difference in the dissociation efficiencies of the $v = 0$ and $v = 1$ vibrational states, which demonstrates the possibility of detecting a $v = 0 \rightarrow v' = 1$ transition by REMPD.

We use a pulsed laser at $\lambda_d = 213$ nm (Xiton Photonics Impress 213) with average power up to 150 mW, repetition rate $f_{\text{rep}} = 12.5$ kHz and a beam waist radius of 300 μm at the trap center (see Fig. 1(a)). The experimental sequence is depicted in Fig 5(c). After creation and sympathetic cooling of H_2^+ as described in the previous Section, we apply the photodissociation laser for the variable duration $\Delta t_d = 0...10$ s. To ensure that losses related to background gas collisions are identical for data points with different Δt_d, we add a waiting time $\Delta t_w = 0...10$ s before Δt_d, such that the total duration of one experiment is always $\Delta t_w + \Delta t_d = 10$ s. This does not account for possible losses due to the pressure increase stemming from the laser pulses themselves. However, in contradistinction with previous results [17], such losses are negligible here because we use much lower UV powers ($P_d \sim 10 - 20$ mW). This is partly due to the deeper UV wavelength (213 nm instead of 248 nm in Ref. [17]), for which the photodissociation cross-section of the $v = 1$ level is much higher. Another reason is that the sympathetically cooled H_2^+ ions are localized in a smaller volume in the vicinity of the trap center, allowing a better overlap with the photodissociation laser.

We measure the ion signal before (S_{ini}) and after (S_{fin}) applying the photodissociation laser, as explained in Sec. IV. From this we deduce the survival probability $p_s(\Delta t_d, \eta) = S_{\text{fin}}/S_{\text{ini}}$ after a given photodissociation duration Δt_d. In order to remove the effect of ion losses, the experiment is repeated without dissociation laser to measure the background survival probability p_{bg}, and we finally obtain a normalized signal $F(\Delta t_d, \eta) = p_s(\Delta t_d, \eta)/p_{\text{bg}}$.

These measurements have to be repeated to get sufficient statistics. In order to reduce the measurement time, Be^+ ions are loaded only when necessary. We proceed in the following way: at the end of the experimental sequence, any remaining H_2^+ and H_3^+ ions are removed from the trap by resonant excitation of the secular motion. This way, we obtain a pure Be^+ crystal and can repeat the experiment by again creating H_2^+ via REMPI. When the number of Be^+ ions has dropped below about half of its initial value, additional Be^+ ions are loaded into the trap via electron-impact ionization.

During operation of the molecular beam source, the Be^+ ions typically have a lifetime of 15 minutes. In addition, a large part of the losses occur through reactive formation of BeH^+ ions and can be reversed using photodissociation by the 213 nm laser [35].

A. Model of the photodissociation dynamics

Since the crystallized H_2^+ ions have very small motional amplitudes, they experience a nearly constant intensity during their interaction with the photodissociation laser. This allows a significantly simplified model of the photodissociation to be used compared to our previous work [17]. For ions in the vibrational state v and located at the beam focus, the survival probability after $N_p = \Delta t_d \times f_{\text{rep}}$ laser pulses is

$$p_{d,v}(\Delta t_d, \eta) = \exp\left[-\eta N_p \frac{2\lambda_d E_p \sigma_v}{\pi h c w_0^2}\right] . \qquad (2)$$

E_p is the pulse energy (measured at the output of the laser), σ_v the dissociation cross section for state v, $w_0 = 300$ μm the $1/e^2$ beam waist radius and h is the Planck constant. The values of σ_v for $v = 0, 1, 2$ are $\{5.355, 386.3, 4787\} \times 10^{-25}$ m^2 at 303 nm [24]. The parameter η accounts for losses at 213 nm on the two

mirrors used to steer the beam (≈5% each), losses on the uncoated focusing lens (8%) and for imperfect overlap of the laser beam with the H_2^+.

To illustrate the latter point, let us consider an H_2^+ ion string of length $2l = 1$ mm parallel to the trap axis. For perfect alignment, i.e. if the photodissociation beam axis crosses the middle of this string, in view of the 28.5° angle between the beam and the trap axis (see Fig. II) the overlap factor is expected to vary between 1 at the center, and $e^{-2(l\sin(28.5°))^2/w_0^2} = 0.28$ at each end of the string, with an average value approximately given by

$$\frac{1}{2l}\int_{-l}^{l} e^{-2(r\sin(28.5°))^2/w_0^2} dr = 0.70.$$

Including the effect of optical losses, one gets $\eta \simeq 0.92 \times 0.95^2 \times 0.70 = 0.58$. Note that the overlap factor may evolve during the depletion of the initial ion string via photodissociation. In the simple model presented here, we will assume η to be fixed.

If the ions are in a mix of vibrational states with populations n_v, the overall survival probability is

$$p_d(\Delta t_d, \eta) = \sum_v n_v p_{d,v}(\Delta t_d, \eta)\,. \tag{3}$$

Due to collisions with background gas, the survival probability without the dissociation laser after $\Delta t_w = 10$ s is $p_{\rm bg}$, measured to be ≈ 85%. The survival probability with the dissociation laser is

$$p_s(\Delta t_d, \eta) = p_{\rm bg} \times p_d(\Delta t_d, \eta), \tag{4}$$

so that the normalized ion signal is

$$F(\Delta t_d, \eta) = p_s(\Delta t_d, \eta)/p_{\rm bg} = p_d(\Delta t_d, \eta). \tag{5}$$

B. Experimental results

We have measured the remaining ion fraction after a variable time of interaction $\Delta t_d = 0...10$ s with the photodissociation laser of average power $P_d = 9.8$ mW, for ions created in the $v = 0$ (respectively $v = 1$) states by setting the REMPI laser to $\lambda = 302.47$ nm (respectively $\lambda = 295.61$ nm). In addition, a measurement was performed for $v = 1$ at a higher power, $P_d = 22.6$ mW. Results are shown in Fig. 6. We observe a fast decay of the ion population for ions created in the $v = 1$ state, and a much slower decay for ions created in the $v = 0$ state, as expected due to the 72 times smaller dissociation cross-section.

We performed a global fit of the data taken at power $P_d = 9.8$ mW using Eq. 3 with a single free parameter η. The vibrational populations measured in Ref. [22] are incorporated in the fit model. These populations are respectively $n_0 = 0.90$, $n_1 = 0.10$ for $\lambda = 302.47$ nm, and $n_0 = 0.09$, $n_1 = 0.80$, $n_2 = 0.11$ for $\lambda = 295.61$ nm. Note that in the first case, a theoretical calculation of vibrational branching ratios yielded $n_0 = 0.96$, $n_1 = 0.04$ [36].

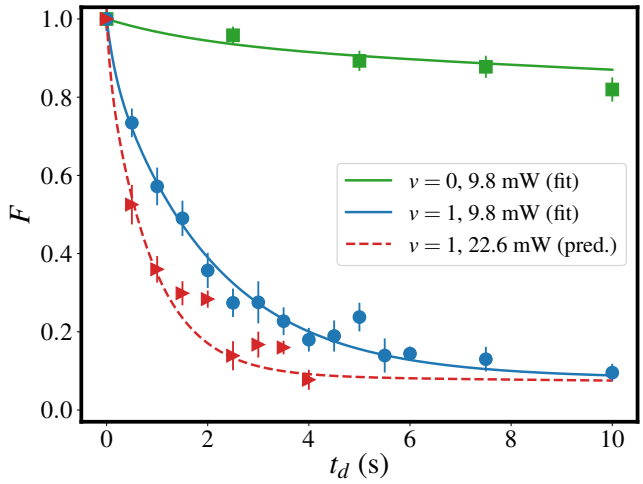

FIG. 6: Dissociation of H_2^+ ions produced by REMPI in the $v = 0$ and in the $v = 1$ states and sympathetically cooled in the linear trap. The normalized remaining ion fraction F (see text) is plotted as a function of the dissociation duration t_d during which the 213 nm laser is applied. Each data point is an average of 6 to 25 measurements. Error bars correspond to the standard deviation. The solid lines indicate a common fit of the data with $P_d = 9.8$ mW using Eq. 3. The dashed line is a prediction for the data with $P_d = 22.6$ mW. Squares: $\lambda = 302.47$ nm, $P_d = 9.8$ mW, circles: $\lambda = 295.61$ nm, $P_d = 9.8$ mW, triangles: $\lambda = 295.61$ nm, $P_d = 22.6$ mW.

The fit is in good agreement with the data for $\eta \approx 0.16$. Using this value, the model correctly predicts the behavior for $P_d = 22.6$ mW. This indicates that both the assumed vibrational populations [22] and the calculated relative dissociation cross-sections [24] provide a good description of the photodissociation dynamics. The value of η is smaller than could be expected from the discussion of the previous section, which we attribute to imperfect alignment of the dissociation beam with the H_2^+ ions. Indeed, it may be explained by a mismatch of about 250 μm in the y direction (see Fig. 1 (c)) with respect to the trap axis, compatible with the uncertainty of our alignment procedure. This may be optimized further in the future.

Our results show that selective dissociation by a 213 nm laser is an effective method to distinguish the vibrational levels $v = 0$ and $v = 1$ in H_2^+, in a characteristic time on the order of 1 s with an average power $P_d = 22.6$ mW.

Since the photodissociation cross-sections depend only weakly on the rotational state, we cannot assess the rotational populations in the ion sample with this method. However, strong rotational selectivity of the REMPI process is expected due to the strong propensity rule of the ionization process [37, 38]. A previous study has observed qualitatively a high level of rotational selectivity (see Fig. 7 in Ref. [22]).

VI. CONCLUSION

By combining (3+1) REMPI from a pulsed H_2 molecular beam, and sympathetic cooling with laser-cooled Be^+ ions, we have demonstrated the production, trapping, and cooling of state-selected H_2^+ ions in the $v = 0$ or $v = 1$ vibrational levels. Differential pumping in the molecular beam apparatus allows a sufficiently low background pressure to be maintained in the trap's vacuum chamber. Deep-UV photodissociation of H_2^+ ions produced by REMPI has yielded results that are compatible with the high vibrational selectivity measured in previous studies, i.e. 90% for the ground vibrational state $v = 0$, and 80% for $v = 1$. Finally, we have shown that photodissociation at 213 nm can be used to detect the excitation of H_2^+ ions from $v = 0$ to $v = 1$ with a rate of approximately 1/s. We have thus demonstrated all the necessary tools to prepare and detect H_2^+ ion samples in a high-resolution spectroscopy measurement.

Finally, the hyperfine state selectivity of the REMPI process [39] is also an interesting topic for further investigations, with the perspective of producing hydrogen molecular ions in a single internal quantum state.

VII. ACKOWLEGMENTS

Thanks are due to A. Douillet for setting-up the 626 nm laser. M.S. acknowledges support by the Austrian Science Fund FWF within the DK-ALM: W1259-N27. This work has been supported by Region Ile-de-France in the framework of DIM SIRTEQ, by the ANR BESCOOL project, grant ANR-13-IS04-0002 of the French Agence Nationale de la Recherche, by the LABEX Cluster of Excellence FIRST-TF (ANR-10-LABX-48-01), within the Program "Investissements d'Avenir" operated by the French National Research Agency (ANR), and by the Initial Training Network COMIQ FP7-PEOPLE-2013-ITN grant 607491.

[1] W. H. Wing, G. A. Ruff, W. E. Lamb, J. J. Spezeski, Observation of the Infrared Spectrum of the Hydrogen Molecular Ion HD^+, Phys. Rev. Lett. **36**, 1488 (1976).

[2] J.-Ph. Karr, L. Hilico, J. C. J. Koelemeij, V. I. Korobov, How to exploit hydrogen molecular ions for improved determination of fundamental constants, Phys. Rev. A **94**, 050501(R) (2016).

[3] V. I. Korobov, L. Hilico, J.-Ph. Karr, Fundamental Transitions and Ionization Energies of the Hydrogen Molecular Ions with Few ppt Uncertainty, Phys. Rev. Lett. **118**, 233001 (2017).

[4] F. Heisse *et al.*, High-Precision Measurement of the Proton's Atomic Mass,Phys. Rev. Lett. **119**, 033001 (2017).

[5] S. Sturm, F. Köhler, J. Zatorski, A. Wagner, Z. Harman, G. Werth, W. Quint, C. H. Keitel, K. Blaum, High-precision measurement of the atomic mass of the electron, Nature **506**, 467 (2014).

[6] S. Schiller, D. Bakalov, V. I. Korobov, Simplest Molecules as Candidates for Precise Optical Clocks, Phys. Rev. Lett. **113**, 023004 (2014).

[7] J.-Ph. Karr, H_2^+ and HD^+: Candidates for a molecular clock, J. Mol. Spectrosc. **300**, 37 (2014).

[8] J. C. J. Koelemeij, B. Roth, A. Wicht, I. Ernsting, S. Schiller, Vibrational Spectroscopy of HD^+ with 2 ppb Accuracy, Phys. Rev. Lett. **98**, 173002 (2007).

[9] U. Bressel, A. Borodin, J. Shen, M. Hansen, I. Ernsting, S. Schiller, Manipulation of Individual Hyperfine States in Cold Trapped Molecular Ions and Application to HD^+ Frequency Metrology, Phys. Rev. Lett. **108**, 183003 (2012).

[10] J. Biesheuvel, J.-Ph. Karr, L. Hilico, K. S. E. Eikema, W. Ubachs, J. C. J. Koelemeij, Probing QED and fundamental constants through laser spectroscopy of vibrational transitions in HD^+, Nature Commun. **7**, 10385 (2016).

[11] S. Alighanbari, M. G. Hansen, V. I. Korobov, S. Schiller, Rotational spectroscopy of cold and trapped molecular ions in the Lamb–Dicke regime, Nature Phys. **14**, 555 (2018).

[12] S. Alighanbari, G. S. Giri, F. L. Constantin, V. I. Korobov, S. Schiller, Precise test of quantum electrodynamics and determination of fundamental constants with HD^+ ions, Nature **581**, 152 (2020).

[13] S. Patra, M. Germann, J.-Ph. Karr, M. Haidar, L. Hilico, V. I. Korobov, F. M. J. Cozijn, K. S. E. Eikema, W. Ubachs, and J. C. J. Koelemeij, Proton-Electron Mass Ratio From Laser Spectroscopy of HD^+ at the Part-per-trillion level, Science, 30 July 2020 (10.1126/science.aba0453).

[14] T. Schneider, B. Roth, H. Duncker, I. Ernsting, S. Schiller, All-optical preparation of molecular ions in the rovibrational ground state, Nature Phys. **6**, 275 (2010).

[15] J. Biesheuvel, J.-Ph. Karr, L. Hilico, K. S. E. Eikema, W. Ubachs, J. C. J. Koelemeij, High-precision spectroscopy of the HD^+ molecule at the 1-p.p.b. level, Appl. Phys. B **123**, 23 (2017).

[16] A. G. Posen, A. Dalgarno, J. M. Peek, The quadrupole vibration-rotation transition probabilities of the hydrogen molecular ion, At. Data and Nucl. Data Tables **28**, 265 (1983).

[17] J.-Ph. Karr, A. Douillet, L. Hilico, Photodissociation of trapped H_2^+ ions for REMPD spectroscopy, Appl. Phys. B **107**, 1043 (2012).

[18] A. K. Hansen *et al.*, Efficient rotational cooling of Coulomb-crystallized molecular ions by a helium buffer gas, Nature **508**, 76 (2014).

[19] S. Schiller, I. Kortunov, M. Hernández Vera, F. Gianturco, H. da Silva, Jr., Quantum state preparation of homonuclear molecular ions enabled via a cold buffer gas: An ab initio study for the H_2^+ and the D_2^+ case, Phys. Rev. A **95**, 043411 (2017).

[20] M. Hernández Vera, F. A. Gianturco, R. Wester, H. da Silva Jr., O. Dulieu, S. Schiller, Rotationally inelastic collisions of H_2^+ ions with He buffer gas: Computing cross sections and rates, J. Chem. Phys. **146**, 124310 (2017).

[21] M. Hernández Vera, S. Schiller, R. Wester, F. Gianturco, Rotationally inelastic cross sections, rates and cooling times for para-H_2^+, ortho-D_2^+ and HD^+ in cold helium gas, Eur. Phys. J. D **71**, 106 (2017).

[22] M. A. O'Halloran, S. T. Pratt, P. M. Dehmer, J. L. Dehmer, Photoionization dynamics of $H_2C^1\Pi_u$: Vibrational and rotational branching ratios, J. Chem. Phys. **87**, 3288 (1987).

[23] X. Tong, A. H. Winney, S. Willitsch, Sympathetic Cooling of Molecular Ions in Selected Rotational and Vibrational States Produced by Threshold Photoionization, Phys. Rev. Lett. **105**, 143001 (2010).

[24] F. von Busch, G. H. Dunn, Photodissociation of H_2^+ and D_2^+: experiment.Physical Review A **5**, 1726 (1972).

[25] S .T. Pratt, P. M. Dehmer, J. L. Dehmer, Photoionasation of excited molecular state H_2 $C^1\Pi_u$, Chem. Phys. Lett. **105**, 28 (1984).

[26] J. H. Posthumus, B. Fabre, C. Cornaggia, N. de Ruette, X. Urbain, Laser-Intensity Dependent Vibrational Excitation and Alignment of Molecular Ions in the Ultrafast Multiphoton Regime, Phys. Rev. Lett. **101**, 233004 (2008).

[27] S. W. Allendorf, A. Szöke, High intensity multiphoton ionization of H_2, Physical Review A **44**, 518 (1991).

[28] X. Urbain, private communication.

[29] D. Irimia, R. Kortekaas, M. H. M. Janssen, In situ characterization of a cold and short pulsed molecular beam by femtosecond ion imaging, Phys. Chem. Chem. Phys. **11**, 3958 (2009).

[30] K. Mølhave, M. Drewsen, Formation of translationally cold MgH^+ and MgD^+ molecules in an ion trap, Physical Review A **62**, 011401(R) (2000).

[31] S. Willitsch, Coulomb-crystallised molecular ions in traps: methods, applications, prospects, Int. Rev. Phys. Chem. **31**, 175 (2012).

[32] J. Heinrich, Trapped and laser-cooled Be^+ Ions for H_2^+ Spectroscopy, PhD Thesis, (Sorbonne Université, Paris, 2018).

[33] A. C. Wilson et al., A 750-mW, continuous-wave, solid-state laser source at 313 nm for cooling and manipulating trapped $^9Be^+$ ions, Applied Physics B **105**, 741 (2011).

[34] Z. Meir, G. Hegi, K. Najafian, M. Sinhal, S. Willitsch, State-selective coherent motional excitation as a new approach for the manipulation, spectroscopy and state-to-state chemistry of single molecular ions, Faraday Discuss. **217**, 561 (2019).

[35] B. C. Sawyer, J. G. Bohnet, J. W. Britton, J. J. Bollinger, Reversing hydride-ion formation in quantum-information experiments with Be^+, Physical Review A, **91**, 011401(R) (2015).

[36] S. N. Dixit, D. L. Lynch, V. McKoy, Three-photon resonant four-photon ionization of H_2 via the $C^1\Pi_u$ state, Phys. Rev. A **30**, 3332 (1984).

[37] V. Q. Tran, Towards High Precision Spectroscopy of Hydrogen Molecular Ions H_2^+ and HD^+ : Theory and Experiment, PhD Thesis, (Université Pierre et Marie Curie, Paris, 2013).

[38] S. N. Dixit, V. McKoy, Theory of resonantly enhanced multiphoton processes in molecules, J. Chem. Phys. **82**, 3546 (1985).

[39] M. Germann, S. Willitsch, Fine- and hyperfine-structure effects in molecular photoionization. II. Resonance-enhanced multiphoton ionization and hyperfine-selective generation of molecular cations, J. Chem. Phys. **145**, 044315 (2016).